Interfacial Charge-Spin Coupling: Injection and Detection of Spin Magnetization in Metals

Mark Johnson and R. H. Silsbee
Laboratory of Atomic and Solid State Physics, Cornell University, Ithaca, New York 14853
(Received 1 July 1985)

The strong inequivalence of spin-up and spin-down subbands in a ferromagnet causes a coupling between the charge and spin transport across the interface of a ferromagnetic and a contiguous paramagnetic metal. This allows the use of sensitive electronic measurements to probe spin transport. Application of small static magnetic fields results in a Hanle effect which permits determination of the spin-relaxation time T_2. The unique features of the method should make it applicable to a wide range of studies.

PACS numbers: 07.58.+g, 72.15.−v, 73.40.−c

We have demonstrated, for the first time, the concept that a coupling between electronic charge and spin exists at an interface between a ferromagnetic and a paramagnetic metal. Not only does this imply that a magnetic current can be created from an electric current, but more important, a nonequilibrium magnetization in a paramagnet can be detected as an electric voltage. Together, this means that one can "tag" electrons with a magnetic moment, and detect the tagged particles at other positions in the material. We prove the usefulness of this by presenting a new, nonresonance technique to measure the spin-relaxation time T_2 of conduction electrons.[1] Usually, T_2 is studied by the transmission electron-spin-resonance (TESR) technique at microwave frequencies and kilogauss fields. The new method may be performed in very small fields, which renders it applicable to systems that are altered or destroyed by high magnetic fields.

Consider an experiment in which one injects spin-polarized electrons into a metal at position $x=0$. These electrons will diffuse a distance $\delta_s=\sqrt{2}DT_2$, where D is the electron diffusion constant, before losing memory of their initial polarization via a spin-relaxation event characterized by the time T_2. The signal at a "spin-detector" probe will fall off exponentially with distance from the injector, and the experimental measurement of the signal amplitude versus probe separation gives a direct measure of δ_s. Alternatively, the Hanle effect, familiar in optical pumping, may be used to measure T_2: The spin magnetization may be destroyed by application of a transverse magnetic field which causes precession of the moments. The field effectively randomizes the spins, because spins injected into the metal at different times in the past have accumulated different phase angles. The characteristic field for destruction of the polarization is $(\gamma T_2)^{-1}$, where γ is the spin gyromagnetic ratio.

The key is to find a means of spin, or magnetization, injection and detection. The solution to the injection problem is conceptually simple, and was proposed by Aronov.[2] Suppose an electric current is driven from a ferromagnetic metal into the paramagnetic metal of interest. If the Fermi surface in the ferromagnetic metal were entirely within one spin subband, then the current would be carried solely by electrons of that spin orientation [Fig. 1(a)]. Magnetization would be injected into the metal at a rate proportional to the electric current. For a real ferromagnetic, the Fermi surface will contain both spin bands, but in a substantial imbalance [Fig. 1(b)]. The reduced efficiency of magnetization injection is described by a phenomenological coefficient $\eta<1$. Associated with the transfer across the interface of each electric charge e is the transport of a magnetization $\eta\beta$, where β is the Bohr magneton. If relaxation at the interface is neglected, then the injected magnetization current I_m associated with an electric current I_e is trivially argued to be

$$I_m=\eta\beta I_e/e\ . \tag{1}$$

Meservey, Paraskevopoulos, and Tedrow[3] have studied the tunneling characteristics of a superconducting film—oxide barrier—ferromagnetic metal tunnel junction to demonstrate spin polarization caused by this mechanism. They have measured values of η in the range 0.1 to 0.5. The injector also serves as spin polarizer. The injected spin polarization is parallel (or possibly antiparallel) to the magnetization of the ferromagnetic metal.

The detector is another junction between a ferromagnet

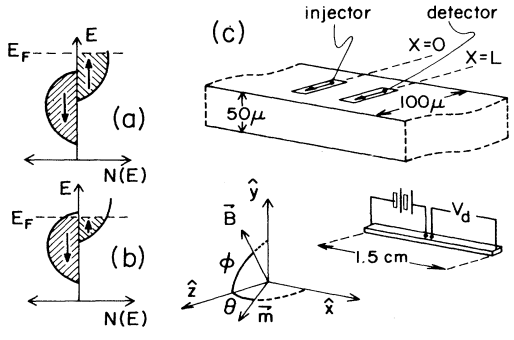

FIG. 1. Overidealized Stoner ferromagnet with (a) a full subband and (b) inequivalent subbands. (c) The geometry of the experiment.

and the sample; its mode of operation is less apparent. If there is a nonequilibrium magnetization M in the paramagnetic metal in the vicinity of the detector, an open-circuit voltage will be developed across the interface of magnitude

$$V=\eta\beta M/\chi e\ , \tag{2}$$

where χ is the magnetic susceptibility of the paramagnet. Formally, this can be derived from Eq. (1) as an Onsager relation among cross coefficients in a linear-response formalism.[4] It also follows for a simple model case, as shown in the work of Silsbee,[5] where the detector was first proposed. The detector serves as a spin analyzer. The detected signal is proportional to the projection (or possibly its negative) of the nonequilibrium magnetization in the paramagnet onto the magnetization of the ferromagnetic detector.

The crux of the experiment described here is the coupling between the charge and spin transport across the interface between a ferromagnetic and a paramagnetic metal. It is caused by the strong inequivalence of spin subbands in a ferromagnet, and allows the use of highly sensitive electronic measurements to probe spin transport and relaxation.

Figure 1(c) depicts the geometry of the experiment. An electric current (~ 30 mA) is passed through the injector and the voltage V_d induced at the detector (typically tens of picovolts) is measured. Note that there is no IR drop from the detector to its ground because there is no net current in the region $x>0$.

We demonstrate the physics of the technique by a one-dimensional random-walk model, similar to the argument Lewis and Carver[6] used to illustrate TESR. A one-dimensional model is valid for $\delta_s > L$ *or* $L >$ sample thickness, a condition satisfied for all but the highest-temperature data set.[4] Spin-polarized electrons are injected in steady state at $x=0$ and eventually relax by a T_2 process. We neglect transverse motion and assume that each electron undergoes a random walk along the x axis. Every τ seconds it moves $l=v_F\tau$, where v_F is the Fermi velocity, either forward or backward. Whenever an electron is at $x=L=pl$ it has a small probability of exiting from the bar through the detector. For this sample of electrons, we plot the distribution of times spent in the bar in Fig. 2. Parameters for results presented later are $\tau=9$ psec, $l=17$ μm, $L=50$ μm, and $p\sim 3$. In the absence of relaxation, the probability $P_{n,p}$ is just the number of ways to get to $x=pl$ in n steps, i.e., the binomial coefficient ${}_nC_{(n+p)/2}$, divided by 2^n:

$$P_{n,p}=\binom{n}{(n+p)/2}2^{-n},\quad n+p \text{ even},$$
$$=0,\quad n+p \text{ odd}.$$

The peak probability occurs at around nine steps as expected for a random walk. There follows a long tail that eventually falls off as $n^{-1/2}$; it takes a long time for electrons to diffuse away from the origin in a one-dimensional bar. In the presence of relaxation there is a probability per step of τ/T_2 (0.001, for the results below) that a spin gets randomized by its collision and is lost to the system. The probability that a spin-polarized electron arrives at the detector after n steps without relaxation is reduced from $P_{n,p}$ by $\exp(-n\tau/T_2)$ and is also plotted in Fig. 2 as $P'_{n,p}$.

To determine the effect of an imposed magnetic field parallel to $\hat{y}$, we suppose that the injected electrons are polarized along $\hat{z}$ and the detector is a magnetization analyzer with orientation along $\hat{z}$ as well. A moment that points at angle θ to $\hat{z}$ will register a magnetization $\propto\cos\theta$. An external field along $\hat{y}$ will cause every spin to precess through a phase angle of $\delta\theta=\gamma B\tau$ in each step. The signal of the analyzer in a static field B is the sum of contributions of all the electrons, weighted by the probability $P'_{n,p}$ that they started from the injector n steps earlier, and multiplied by the precession factor $\cos(\gamma Bn\tau)$:

$$\text{Signal}\propto\sum e^{-n\tau/T_2}\,{}_nC_{(n+p)/2}2^{-n}\cos(\gamma Bn\tau)\ . \tag{3}$$

The signal as a function of field, calculated numerically from Eq. (3) with $p=3$, is plotted in Fig. 2(c). In this example, the detector is well within a spin-diffusion length, given (in one dimension) as $\delta_s=(2lv_FT_2)^{1/2}$, of the injector. In TESR this is known as the "thin limit." The moments dephase before the net magnetization has precessed and the feature width is characterized by T_2, which shapes the tail in Fig. 2(a). For larger probe separations and shorter mean free paths (higher temperature) one enters the regime $\delta_s > L$. This is known as the "thick limit," in which the detector preferentially samples electrons with relatively long travel times, and the Hanle signal

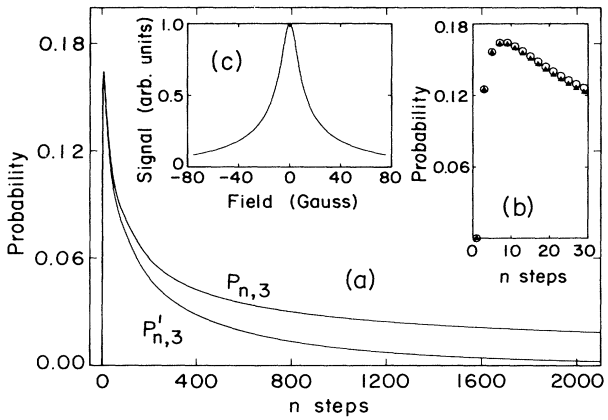

FIG. 2. (a) The unnormalized probability $P_{n,3}$ that a moment took n steps to arrive at the detector located at $L=3l$ in the absence of relaxation. $P'_{n,3}$ is the reduced probability in the presence of relaxation. (b) A detail of (a) showing the distribution of arrival times. (c) Signal calculated numerically from Eq. (3).

develops side lobes. The width and shape become influenced by the arrival-time distribution [Fig. 2(b)] as well as the decay time, T_2.

We have presented this model because there is a clear physical interpretation of the signal: It is the Fourier transform of the probability $P'(t)$ of finding an unrelaxed moment at the detector at time t. One can use Eqs. (1) and (2), take the continuum limit of ${}_nC_{(n+p)/2}$, and perform the Fourier transform to derive an explicit functional form[4] that predicts the signal shape and amplitude with only two independent fitting parameters, η and T_2. This is equivalent to solving the Bloch equations with a diffusion term.[4]

Note that a field applied along $\hat{\mathbf{x}}$ would generate the same shape signal. However, a field applied along $\hat{\mathbf{z}}$ exerts no torque on the spins; they will not precess, and there will be no quenching of the signal by the applied field. Instead, one expects a signal that is independent of field strength. For the general case of a field applied at angle ϕ with respect to the magnetization direction $\hat{\mathbf{z}}$, the field-dependent signal should vary as $\sin^2\phi$.

The paramagnetic metal in this experiment was pure aluminum with a bulk residual resistivity ratio (RRR) at 4 K of about 10^4 before processing. It was cold rolled, annealed, and sliced into a bar 50 μm by 100 μm by 1.5 cm. This was fixed to a sapphire substrate and coated with a 1-μm layer of polyimide. Windows 15×40 μm^2 were photolithographically defined and chemically etched through this insulating layer to expose the surface of the aluminum. The surface was cleaned with an argon-ion mill, and a thin film ($\sim$650 Å) of Permalloy was electron-beam evaporated at a base pressure of 10^{-7} Torr. Gold was evaporated over the Permalloy to inhibit oxidation. Indium wires were cold welded to these junctions and led to the injecting and detecting circuits. The resistance of the junctions is estimated to be less than a few milliohms, but we do not believe them to be clean, metal-to-metal interfaces. The samples had a RRR of $\sim$1100 after processing; the mean free path is dominated by surface scattering. The detector was a SQUID picovoltmeter, used with an ac bridge and a lockin at 4 Hz. Sensitivity was a few picovolts.[4] For $\eta=0.07$, this corresponds to a *nonequilibrium* spin imbalance in the aluminum of 1 spin in 10^{11} (i.e., $\Delta n/n\approx10^{-11}$), or to the imbalance produced in *equilibrium* (Zeeman splitting) by an applied field of 10 mG![4]

The magnetization of thin ferromagnetic films remains nearly in the plane of the films for applied fields of any orientation as long as the applied field is small in magnitude compared with the $4\pi M$ of the film. The films used in our experiment show substantial in-plane anisotropy of unknown origin. Once established in the $-\hat{\mathbf{z}}$ direction by application of a large applied field along $-\hat{\mathbf{z}}$, the magnetization appears to be stable against reversal up to an opposing field (along $\hat{\mathbf{z}}$), B_0, of about 100 G. It is stable against large in-plane rotation for applied fields in the $\hat{\mathbf{x}}$ direction less than 40 G. In a typical experiment, a field of a few hundred gauss is applied along $\hat{\mathbf{z}}$ to define the magnetization of injector and analyzer parallel to each other. B_z is then reduced to zero and the field is swept along $\hat{\mathbf{x}}$ or $\hat{\mathbf{y}}$, or at angle ϕ from $\hat{\mathbf{z}}$ in the y-z plane. The component of field along $-\hat{\mathbf{z}}$ is always less than B_0, so that the initial alignment of injector and analyzer is preserved.

The $\hat{\mathbf{x}}$ and $\hat{\mathbf{y}}$ sweeps show a signal of the predicted shape, with a reasonable width and amplitude. Sweeps on a control sample (no ferromagnetic film) showed no Hanle signal. The predicted $\sin^2\phi$ dependence of the Hanle-signal amplitude as a function of orientation of applied field is confirmed in the inset of Fig. 3. A typical $\hat{\mathbf{z}}$ sweep is shown in Fig. 3. The magnetization of the films is established along $-\hat{\mathbf{z}}$, and the field is swept from negative to positive. Note there is no Hanle effect around $B=0$, as predicted. There is, however, a dramatic change in signal at $B_{0,1}$, with recovery to the original signal at $B_{0,2}$. At $B_{0,1}$ the injector (or detector) magnetization has reoriented by 180° and points along $+\hat{\mathbf{z}}$, resulting in a reversal of sign of the spin-coupled signal. At $B_{0,2}$ the detector (or injector) has flipped its orientation as well; now both are aligned along $+\hat{\mathbf{z}}$ and the original signal is recovered. This interpretation was confirmed by halting a $\hat{\mathbf{z}}$ sweep between $B_{0,1}$ and $B_{0,2}$, reducing the field to zero, and then sweeping B along $\hat{\mathbf{y}}$. The Hanle signal is observed, as in Fig. 1(c), but with opposite sign, a dip rather than a peak.

As a more detailed test of the interpretation, data were taken on several samples of different probe separations, over the temperature range 4 to 55 K, and fitted by the function described above. Two examples of data and fits are shown in Figs. 4(a) and 4(b). The former is an $\hat{\mathbf{x}}$ sweep in the limit $\delta_s<L$. The latter is a $\hat{\mathbf{y}}$ sweep in the limit $\delta_s>L$. Note the appearance of side lobes beyond the central peak, as predicted. The small asymmetry in line shape is readily explained by a generalization which includes the effect of imperfect alignment of polarizer and analyzer.[4]

Values of η for two samples are 0.060 ± 0.008 and

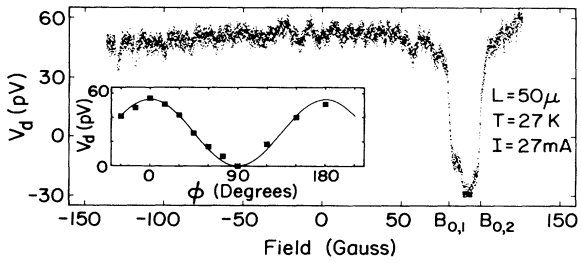

FIG. 3. Sample Walrus7; typical $\hat{\mathbf{z}}$ sweep, from negative to positive field; zero voltage is arbitrarily determined by the bridge. Inset: Observed Hanle-signal amplitude as a function of orientation angle ϕ of magnetic field.

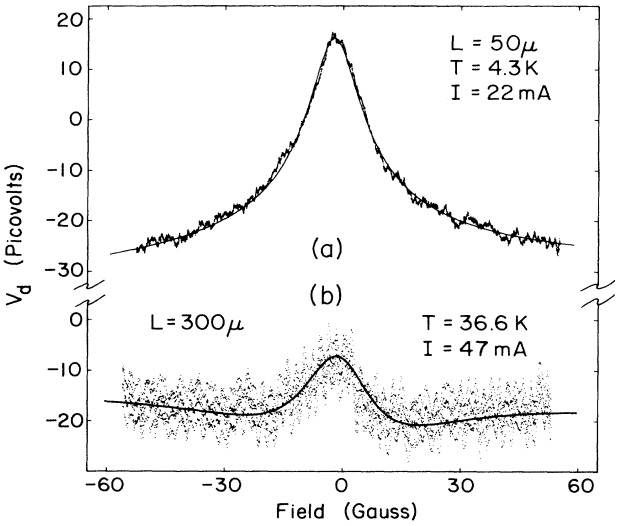

FIG. 4. (a) Sample Walrus7, $\hat{\mathbf{x}}$ sweep and fit, in the thin limit. $\delta_s = 450\ \mu\text{m} \gg 50\ \mu\text{m} = L$. (b) Sample Walrus6, average of three $\hat{\mathbf{y}}$ sweeps and fit, in the thick limit. $\delta_s = 170\ \mu\text{m} < 300\ \mu\text{m} = L$.

0.081 ± 0.010. There is no apparent systematic temperature variation. Note, however, that these values of η are significantly less than Meservey, Paraskevopoulos, and Tedrow have reported. A superconducting conductance measurement (at 1 K) of a junction identical to the sample's showed that it was not a good tunnel junction. Interpretation of this discrepancy in η's will require a more detailed characterization of the junctions.

As a final test of the model, the values of T_2 determined by the fits are compared with values of T_2 measured by the TESR method. To minimize the effect of g anisotropies in aluminum we compare with the lowest-frequency data available. Lubzens and Schultz[7] have studied TESR of a 40-μm-thick foil of aluminum (RRR = 1600) at 1.3 GHz. Figure 5 shows a comparison of the two sets of T_2's. Contributions to the linewidth come from spin-flip scattering with impurities, sample surfaces, and phonons. The first two account for the residual width at low temperature. This width is subtracted from the higher-temperature values in order to isolate the temperature dependence, $T_{2,\text{ph}}$.

Novel features of the technique include the ability to measure T_2 in zero field, avoiding the line broadening by g anisotropies that makes TESR unobservable in many

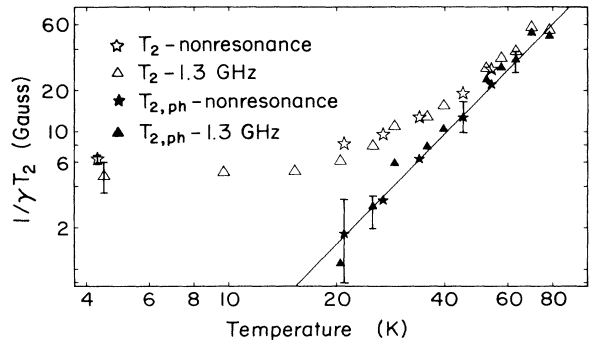

FIG. 5. Comparison of relaxation times between the new, nonresonance method, and TESR at 1.3 GHz.

metals; applicability to the study of spin transport in superconductors and spin-glasses; and a simple experimental geometry in which to measure surface relaxation.[8] The inverse proportionality of the signal to sample cross-sectional area suggests applications to very small-size systems, which are inaccessible to conventional ESR. Another obvious extension is to single-crystal and tunneling studies of the interfacial coupling efficiency η.

One of us (M.J.) wishes to acknowledge gratefully the technical assistance of J. Lebens and D. McQueeney, a useful conversation with A. Janossy, and the use of the National Research and Resource Facility for Submicron Structures. This work has been supported by the Cornell Materials Science Center, through National Science Foundation Grant No. DMR-8217227A-01.

[1]In small fields, there is no distinction between transverse (T_2) and longitudinal (T_1) relaxation events.

[2]A. G. Aronov, Pis'ma Zh. Eksp. Teor. Fiz. **24**, 37 (1976) [JETP Lett. **24** 32 (1976)].

[3]R. Meservey, D. Paraskevopoulos, and P. M. Tedrow, Phys. Rev. Lett. **37**, 858 (1976).

[4]Mark Johnson and R. H. Silsbee, to be published.

[5]R. H. Silsbee, Bull. Magn. Reson. **2**, 284 (1980).

[6]Richard B. Lewis and Thomas R. Carver, Phys. Rev. **155**, 309 (1967).

[7]D. Lubzens and S. Schultz, Phys. Rev. Lett. **36**, 1104 (1976).

[8]D. M. Eigler and S. Schultz, Phys. Rev. Lett. **54**, 1185 (1985).